Science Advances
AAAS

advances.sciencemag.org/cgi/content/full/6/8/eaay3178/DC1

Supplementary Materials for

Intrinsic disorder controls two functionally distinct dimers of the master transcription factor PU.1

Suela Xhani, Sangchoon Lee, Hye Mi Kim, Siming Wang, Shingo Esaki, Van L. T. Ha, Mahtab Khanezarrin, Giselle L. Fernandez, Amanda V. Albrecht, James M. Aramini, Markus W. Germann*, Gregory M. K. Poon*

*Corresponding author. Email: gpoon@gsu.edu (G.M.K.P.); mwg@gsu.edu (M.W.G.)

Published 21 February 2020, *Sci. Adv.* **6**, eaay3178 (2020)
DOI: 10.1126/sciadv.aay3178

This PDF file includes:

Table S1. DNA binding and self-association equilibrium constants of PU.1 constructs.

DNA-binding data was fitted to titration models as detailed in *Materials and Methods*. The choice of fitting with one or two dissociation constants was made based on the magnitude of anisotropy change and statistically by the Fisher's *F*-test on sums of squares at $p = 0.05$. Estimates in μM are given as means ± SE of three or more replicate experiments. n.d., not detectable.

Dissociation constants of 1:1 and 2:1 complexes in the absence of osmolytes or crowders

K_{D1} and K_{D2}, μM	$[Na^+]$, M		
	0.15	0.10	0.05
ΔN117	0.0038 ± 0.0019 7.1 ± 3.3	0.010 ± 0.001 15 ± 5	0.19 ± 0.05
ΔN165	0.0091 ± 0.0015 1.9 ± 0.9	0.036 ± 0.003	0.13 ± 0.02
sΔN117	0.0051 ± 0.0007 6.0 ± 1.3		0.0074 ± 0.0022 3.5 ± 1.8
sΔN165	0.11 ± 0.03 15 ± 9		0.13 ± 0.02 32 ± 24
D_2ΔN117	0.0056 ± 0.0008 6.7 ± 3.2		
D_4ΔN117	0.013 ± 0.004 108 ± 39		
DKCDK monomer	0.013 ± 0.03 2.5 ± 0.4		
DKCDK dimer	3.1 ± 0.9 n.d.		
R232A/R235A	>0.5		

Dissociation constants of 1:1 and 2:1 complexes in the presence of co-solutes

K_{D1} and K_{D2}, M	[Co-solute], % w/v		
	15%	20%	
Ovalbumin	$(3.8 \pm 0.7) \times 10^{-9}$ $(9.5 \pm 1.1) \times 10^{-6}$	$(6.3 \pm 0.6) \times 10^{-9}$ $(3.2 \pm 0.5) \times 10^{-5}$	
	5%	10%	
BSA	$(7.9 \pm 1.5) \times 10^{-11}$ $>10^{-4}$	$(3.0 \pm 1.9) \times 10^{-11}$ $>10^{-4}$	
	10%		10%
PEG 8K	$(1.6 \pm 0.7) \times 10^{-8}$ $(2.1 \pm 1.5) \times 10^{-6}$	Ethylene glycol	$(7.0 \pm 1.6) \times 10^{-9}$ $(6.2 \pm 1.6) \times 10^{-6}$

[NaCl] = 0.15 M

Two-state dissociation constants of ΔN117 and ΔN165 constructs by CD spectroscopy

(Affinities at 0.15 M NaCl unless otherwise indicated)

Construct	K_2, μM
ΔN117 (wildtype)	46 ± 20
sΔN117	≫300
D_2ΔN117	25 ± 3
D_4ΔN117	13 ± 1
ΔN165 (wildtype)	≫800 202 ± 72 (0.05 M NaCl)
sΔN165	n.d.

Table S2. Primers in RT-PCR experiments.

Gene	⇆	Sequence	Amplicon, bp	T_m, °C
pu.1	F	5´-CTC CAG TAC CCA TCC CTG TC-3´	158	64
	R	5´-CGG ATC TTC TTC TTG CTG CC-3´		
csf1ra	F	5´-CAG AGC CTG CTG ACT GTT GA-3´	263	60
	R	5´-TTG CCC TCA TAG CTC TCG AT-3´		
e2f1	F	5´-AAG GGA AGG AGT CTG TGT GG-3´	214	64
	R	5´-CGA AAG TGC AGT TAG AGC CC-3´		
gapdh	F	5´-CGG AGT CAA CGG ATT TGG TCG-3´	225	60
	R	5´-TCT CGC TCC TGG AAG ATG GTG AT-3´		

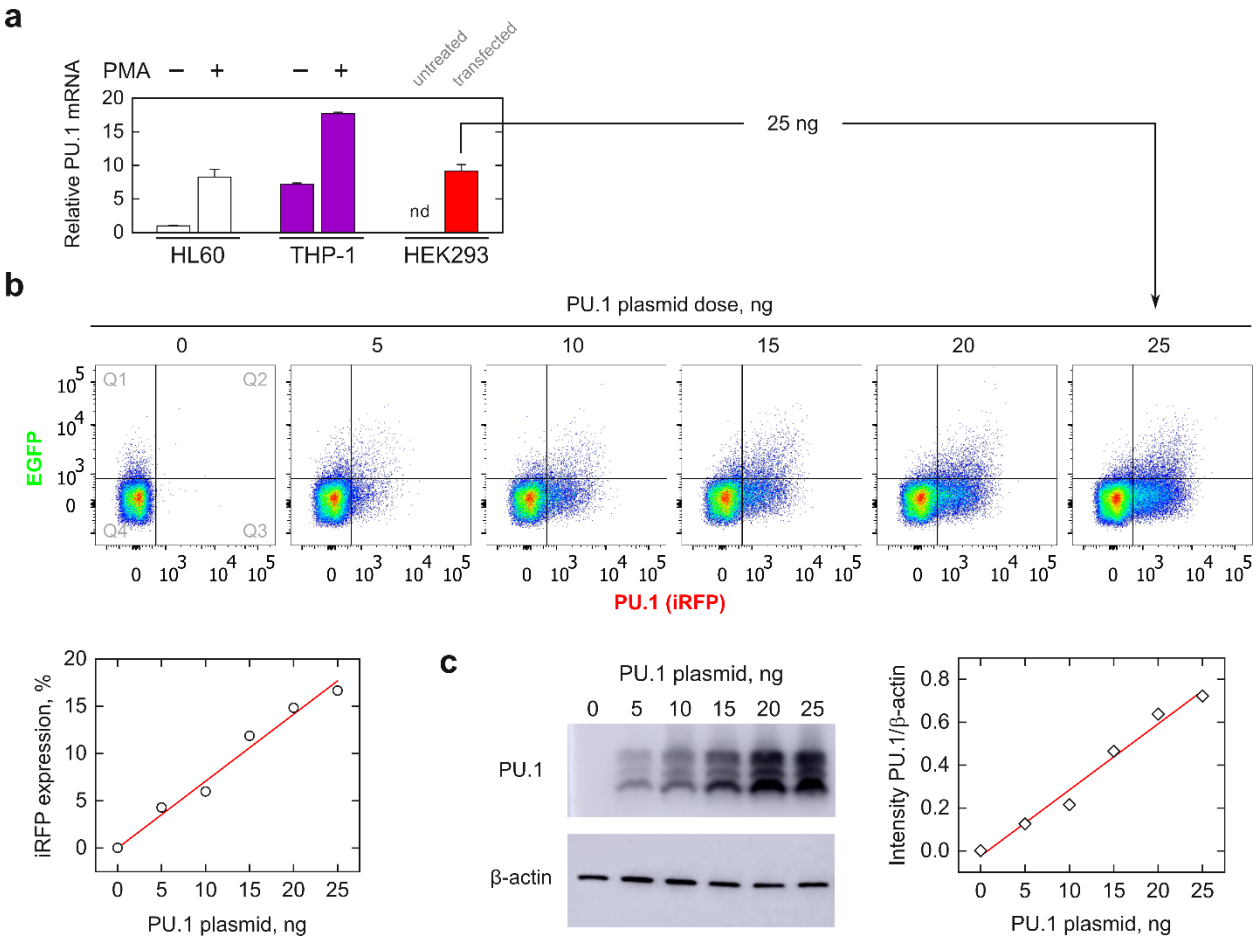

Fig. S1. Calibration of transgenic PU.1 dosage. a, To determine the dosage of PU.1 transgene that would yield physiologically relevant levels of PU.1, transcripts of the *pu.1/Spi1* gene were quantified in two model human myeloid cell lines, under normal proliferative conditions as well as under induction by 16 nM of phorbol 12-myristate (PMA). Consistent with the strong inducibility of PU.1 in primary tissue, PMA induced PU.1 mRNA transcripts in both cell lines. All samples were presented as means ± SE of at least 3 biological replicates relative to *gapdh*. The data establish that a maximum dose of 25 ng (per well of a 24-well plate) of the PU.1 expression plasmid in HEK293 (see *Materials and Methods* in the main text) would yield an expression level comparable to induced HL-60 and non-induced THP-1, but well below levels in that cell line under PMA induction. **b,** We then determined whether 25 ng of the PU.1-expression plasmid would yield a linear dosing range for the λB reporters following transient transfection in HEK293 cells. PU.1 expression was quantified by its co-translating PU.1 iRFP marker by flow cytometry. Cells in quadrant Q2 and Q3 represented PU.1-expressing cells. The sum of their counts were plotted against the plasmid dosage. *Line* represents a linear fit to the data. **c**, To cross-validate the flow cytometric approach, PU.1 abundance was also measured by immunoblotting transfected HEK293 lysates at 10 µg per lane. PU.1 was probed with a rabbit polyclonal antibody (Cell Signaling, #2266) followed by an HRP-coupled mouse anti-rabbit secondary antibody (Santa Cruz). β-actin (loading control) was probed with a mouse monoclonal antibody (Santa Cruz) with an HRP-coupled rabbit anti-mouse secondary antibody (Santa Cruz). Blots were visualized using an Amersham Imager 600 and quantified using ImageJ software.

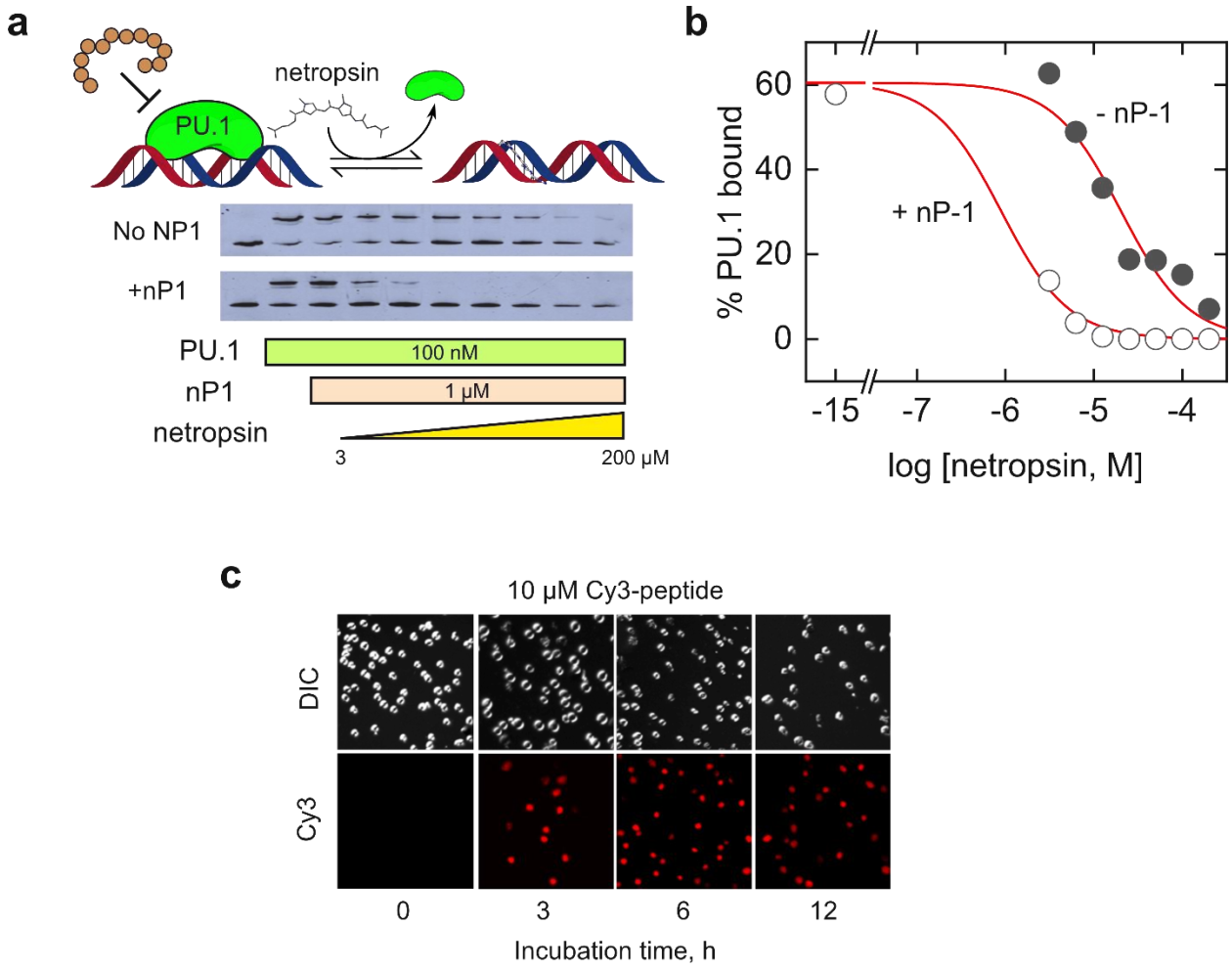

Fig. S2. Characterization of a peptide-based PU.1 inhibitor. a, The synthetic dodecameric peptide nP-1 (Ac-RDYHPRDHTATW-NH_2) inhibited cognate DNA binding by PU.1 in a competitive gel-mobility shift assay using netropsin. Each netropsin-containing lane represented a 2-fold increase in concentration. In the negative control without nP-1, PU.1 was displaced by netropsin binding to the DNA minor groove adjacent to the 5'-GGAA-3' consensus. **b**, Quantification of the mobility shift data shows that nP-1 at 1 μM was highly synergistic with netropsin, reducing the apparent IC_{50} by >20 fold. **c**, Uptake of Cy3-labeled peptide by THP-1 cells at 10 μM, imaged at 63× magnification.

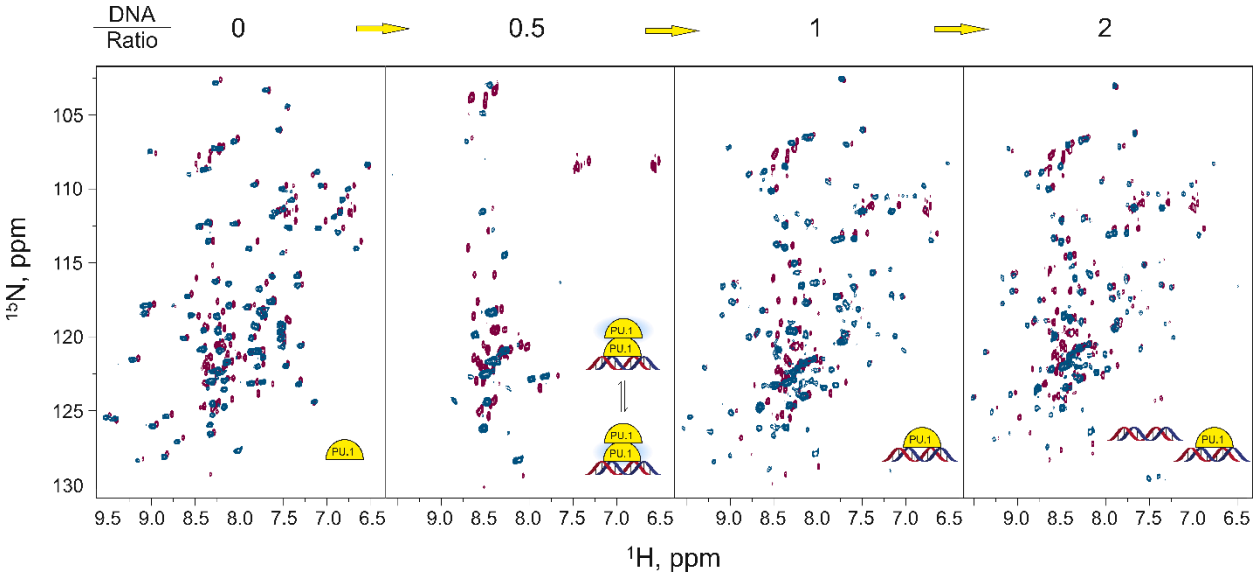

Fig. S3. ^{1}H-^{15}N HSQC-detected titration of ΔN117 and ΔN165 by cognate DNA. ΔN117 is in red, ΔN165 in blue. Conditions were essentially the same as the DOSY titration in Figure 1B (0.15 M NaCl), except uniformly ^{15}N-labeled protein was used at 400 µM.

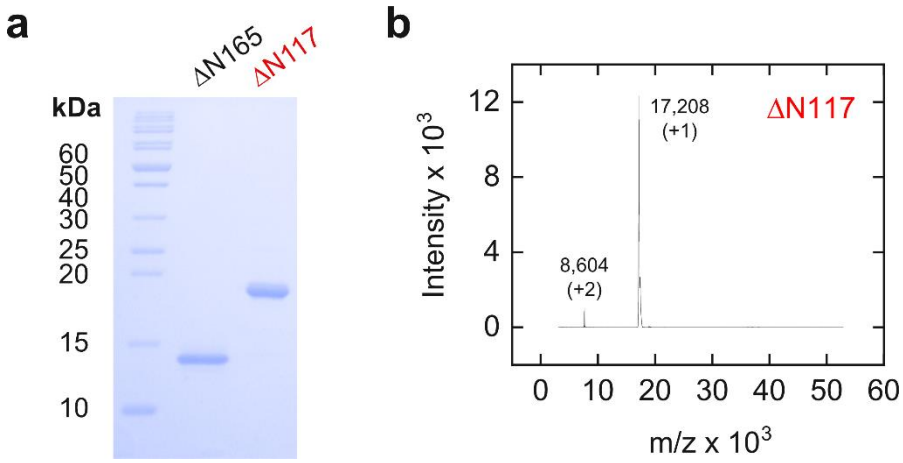

Fig. S4. Purity of recombinant PU.1 constructs. a, One µg of each purified PU.1 construct was resolved in a 15% polyacrylamide gel (29:1) under standard denaturing (0.1% SDS) and reducing conditions (0.5 mM TCEP). **b**, MALDI-ToF mass spectrum of ΔN117.

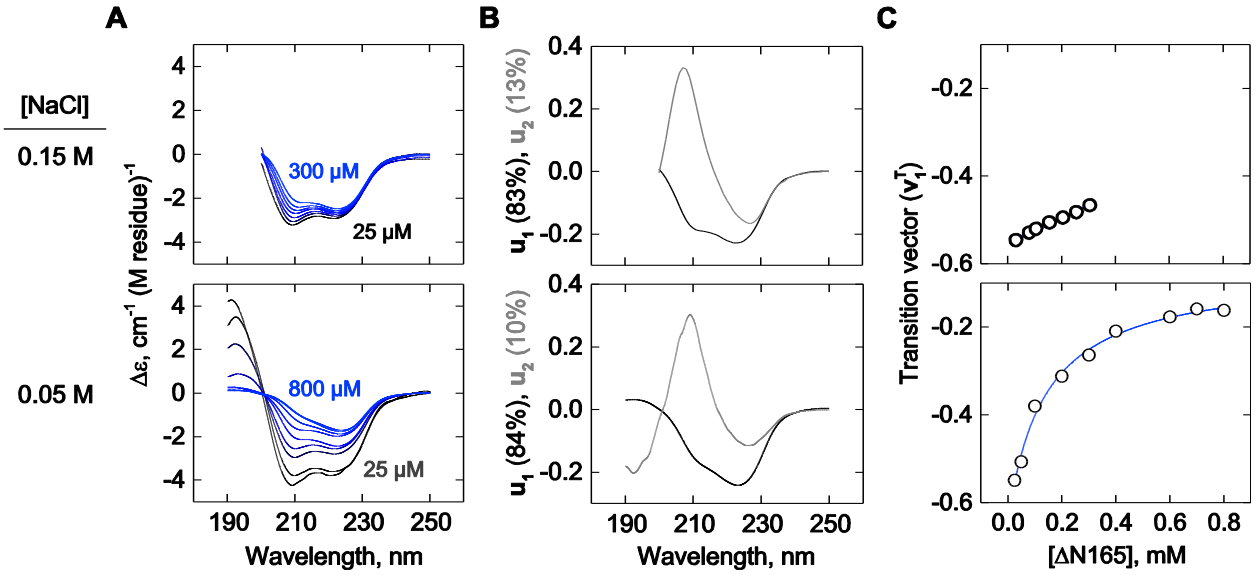

Fig. S5. Spectral analysis of far-UV CD of ΔN165 in 0.15 and 0.05 M NaCl. a, Blank-subtracted, concentration-corrected spectra. Absorption by Cl^- limits the useable ranges of wavelengths and protein concentration in 0.15 M NaCl to those shown. **b**, Following singular value decomposition (see *Materials and Methods* for details), the two most dominant basis vectors in **U**. **c**, Progress curves of the concentration dependence as represented by the transition vectors $\mathbf{V}^{\mathbf{T}}$. The 0.05 M transition was fitted to a two-state dimer. The dissociation constant is 202 ± 72 µM.

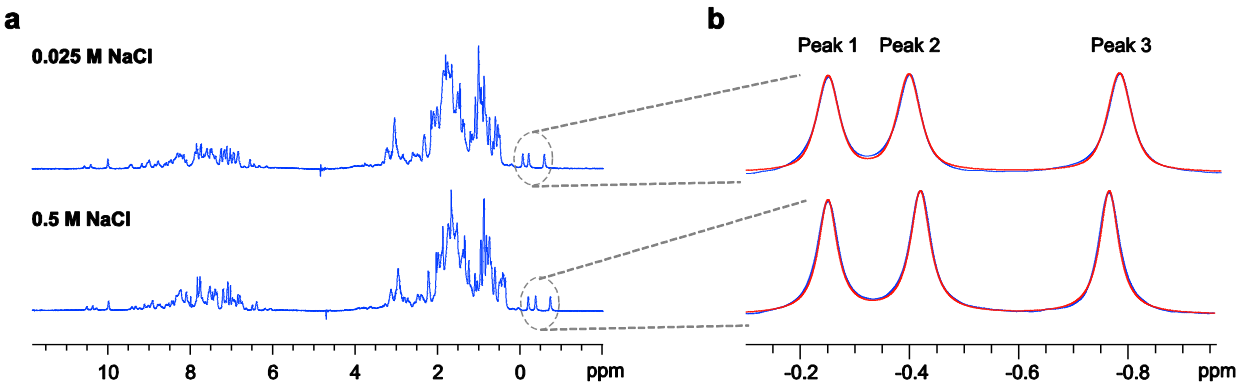

c

	0.25 M NaCl		0.5 M NaCl	
	$\Delta\nu_{½}$, Hz	T^*_2, s	$\Delta\nu_{½}$, Hz	T^*_2, s
Peak 1	24.2 ± 0.2	0.0132 ± 0.0001	21.9 ± 0.1	0.0145 ± 0.0001
Peak 2	25.3 ± 0.2	0.0125 ± 0.0001	22.9 ± 0.1	0.0139 ± 0.0001
Peak 3	27.6 ± 0.2	0.0115 ± 0.0001	21.9 ± 0.1	0.0145 ± 0.0001

Fig. S6. Salt-dependent line broadening of methyl protons in ΔN165. a, Methyl protons located at negative chemical shifts of ^{1}H spectra, acquired at 500 MHz, of identical concentrations (350 μM) of ΔN165 in the presence of 0.025 and 0.5 M NaCl, respectively. **b**, The linewidths, converted to Hz = s^{-1}, were fitted to a sum of Lorentzian peaks (red) from which the full widths at half maximum ($\Delta\nu_{½}$) were estimated by nonlinear regression. **c**, The effective T_2^* for each peak was then computed from

$$T_2^* = \frac{1}{\pi\Delta\nu_{½}} \tag{S1}$$

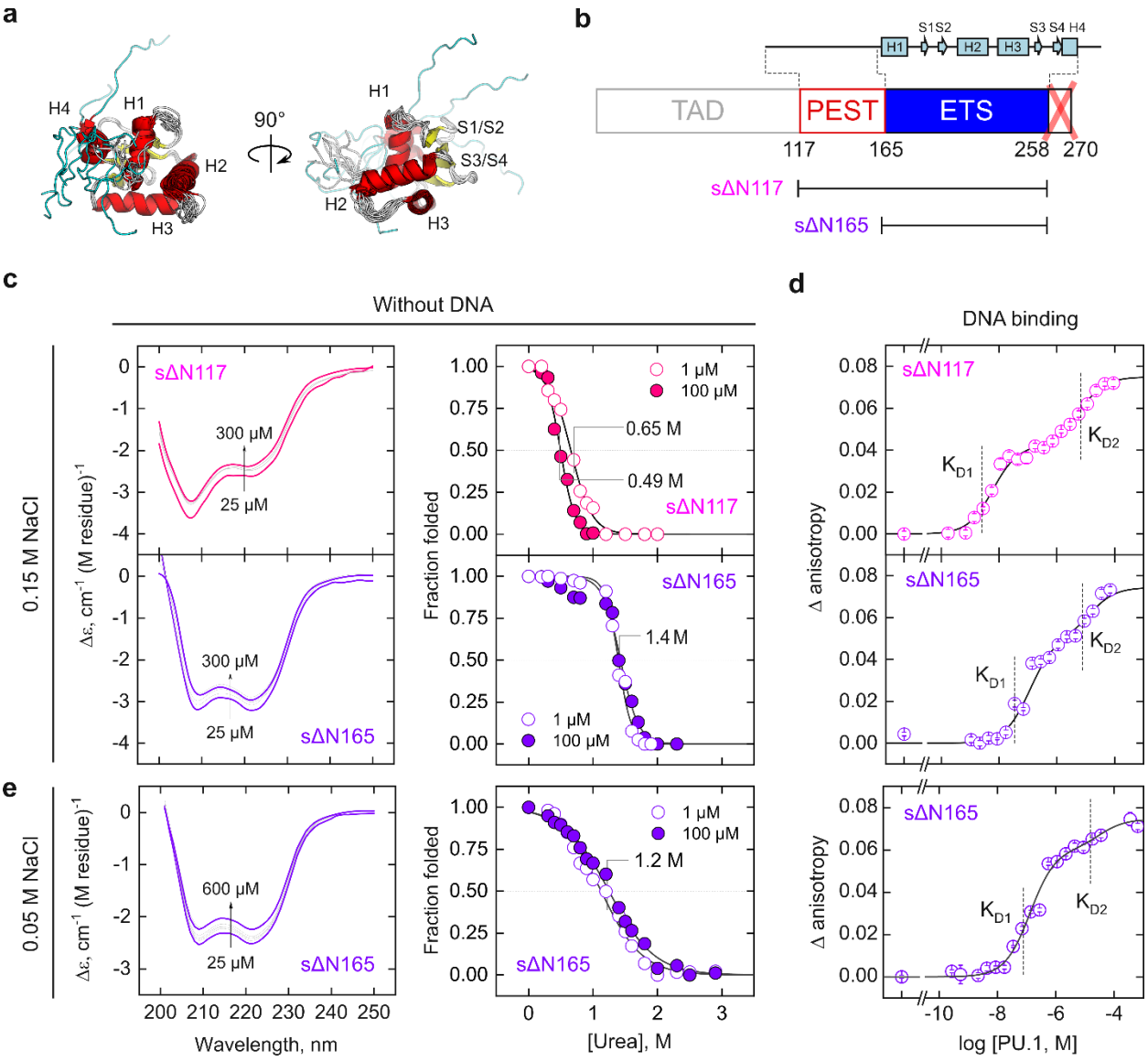

Fig. S7. The short C-terminal IDR is required for DNA-free PU.1 dimerization. a, Superposition of the 10 models in the solution NMR structure of the PU.1 monomer, 5W3G. The C-terminal IDR is colored cyan. **b**, Schematic of PU.1 constructs, sΔN117 and sΔN165, without the C-terminal 12-residue IDR. **c,** Far-UV CD spectra (left) and urea denaturation curves (right) of sΔN117 and sΔN165 at 0.15 M Na^+. The molarity stated represents urea concentrations at 50% unfolding. **d**, Cognate DNA binding by sΔN117 and sΔN165 at 0.15 M Na^+. **e**, Corresponding data for sΔN165 at 0.05 M Na^+. In contrast with ΔN165 (*c.f.* Figures 5a and b), sΔN165 shows negligible propensity for dimerization without DNA but exhibits biphasic DNA binding.

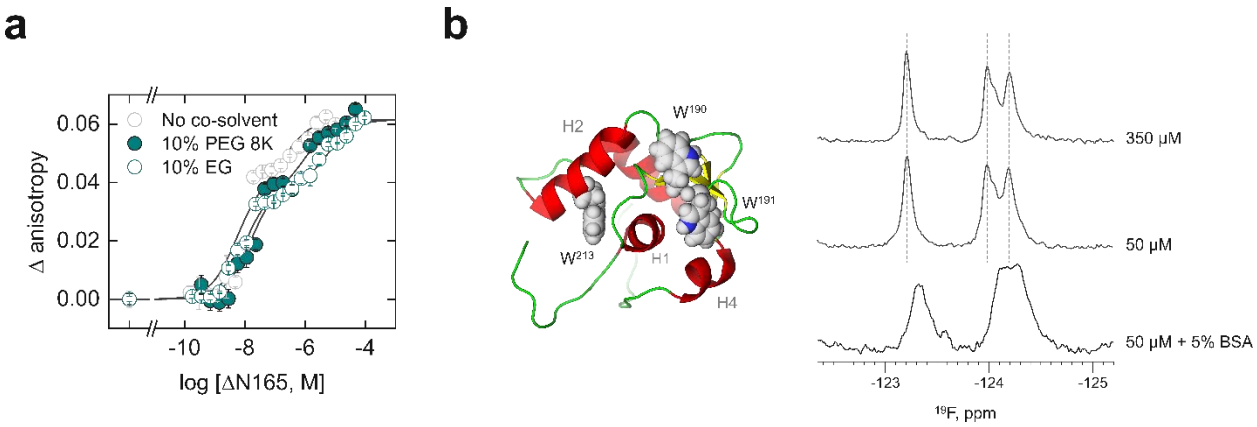

Fig. S8. Effect of macromolecular crowding on dimerization of ΔN165 in the unbound and DNA-bound states. a, Charge-neutral crowding with PEG 8K on cognate DNA binding by ΔN165. Representative titrations in the presence of 10% w/v ethylene glycol (EG) showed destabilization consistent with osmotic stress as previously reported (Poon, J Biol Chem 287, 18297-18307, 2012). The presence of the same mass concentration of polymeric PEG 8K was similar. In both cases and in stark contrast with the acidic crowder BSA, the 2:1 complex was preserved. **b,** ^{19}F NMR reveals conformational perturbations in ΔN165 consistent with unbound dimer formation. The three Trp residues (190, 191, and 213) in ΔN165 were isotopically labeled with 5-fluoroindole in minimal M9 media. Chemical shifts were acquired at 0.15 M Na^+ in D_2O-reconstituted buffer and referenced against the published value for 5-fluoroindole in 90% D_2O (Sarker et al., Biochemistry 55, 3048-3059, 2016). No concentration-dependent chemical shift perturbation (CSP) was detectable at 350 and 50 μM at ΔN165, in contrast with the presence of 5% w/v BSA. Line broadening in the BSA-containing sample was expected due to increased viscosity.